İSTANBUL UNIVERSITY CERRAHPAŞA

ORIGINAL ARTICLE
Electrica 2026; 26: 1-15

Link Performance Prediction of Power Fiber Optic Communication System Based on Attention Mechanism and Convolutional Neural Network Fusion

Yong Zhang, Yan Liu, Chunying Wang, Jiaojiao Dong

State Grid Henan Electric Power Company Information and Communication Branch, Zhengzhou, Henan, China

Cite this article as: Y. Zhang, Y. Liu, C. Wang and J. Dong, "Link performance prediction of power fiber optic communication system based on attention mechanism and convolutional neural network fusion," *Electrica*, 26, 0162, 2026. doi: 10.5152/electrica.2026.25162.

WHAT IS ALREADY KNOWN ON THIS TOPIC?

- *Existing research has applied graph neural networks (GNNs), multi-objective optimization, and AI techniques (e.g., digital twins, 5G edge computing) to power communication systems.*
- *However, current methods struggle to capture both local and global topological features, handle dynamic network changes, or effectively balance multiple optimization objectives.*

WHAT THIS STUDY ADDS ON THIS TOPIC?

- *This study proposes a graph attention residual network–based routing and fault-tolerant scheduling mechanism that adaptively learns node/link importance and integrates multi-scale topological features, improving resilience and performance in dynamic power optical fiber communication systems.*

Corresponding author:
Yong Zhang

E-mail:
yongzhang36@126.com

Received: May 27, 2025
Revision Requested: July 1, 2025
Last Revision Received: August 28, 2025
Accepted: September 7, 2025
Publication Date: January 19, 2026

DOI: 10.5152/electrica.2026.25162

ABSTRACT

In order to enhance the multi-objective optimization capability of power communication transmission networks, the author proposes an optimization method that integrates improved graph neural networks (GNNs) and genetic algorithms (GAs). The model integrates graph convolution and an attention mechanism to construct a multi-output prediction structure, achieving joint optimization of network reliability, transmission delay, and resource utilization. The test results on Institute of Electrical and Electronics Engineers (IEEE) 118 and 300 node systems show that this method significantly outperforms traditional Convolutional Neural Network (CNN) models in terms of network reliability (improved by 9.7%), latency (reduced by 24.7%), and resource utilization (improved by 11.5%). At the same time, the fusion model optimized the convergence algebra by 38% and increased the number of non-dominated solutions by 50%, demonstrating stronger solution space exploration ability and convergence efficiency. (1) Integrating a dynamic attention mechanism (graph attention module) with a residual graph convolution module to prioritize bottleneck links in power networks, unlike GraphCast's fixed attention weights and (2) embedding GNN-derived features into GA initialization, addressing OpenDSS-GA's reliance on random population generation. The research has verified the effectiveness and scalability of this method in large-scale power communication networks, providing new ideas for optimizing complex networks.

Index Terms—Attention mechanism, electric power communication transmission network, genetic algorithm, graph neural network, multi-objective optimization

I. INTRODUCTION

With the rapid development of smart grid and energy Internet, as the core infrastructure supporting power information transmission, the accurate prediction and optimization of the link performance of the power fiber communication system has become the key to ensuring the safe and stable operation of the power grid [1]. The power communication network carries key tasks such as scheduling control, fault protection, and real-time data exchange. Its reliability, latency, and resource utilization directly affect the overall efficiency of the power system [2, 3]. However, power communication networks have the characteristics of complex topology, strong dynamic variability, and multi-objective coupling. Traditional optimization methods face challenges such as low computational efficiency and insufficient solution space exploration ability when dealing with large-scale networks. How to effectively integrate advanced data-driven technology and intelligent optimization algorithms, and break through the limitations of existing models in expressing complex network features, has become a current research focus.

In recent years, significant progress has been made in the optimization research of power communication systems at both theoretical and technical levels. Wang et al. focused on modeling the channel characteristics of spacecraft direct current (DC) power line communication. By analyzing the attenuation and noise characteristics of high-frequency signal transmission, they proposed an adaptive modulation method based on physical layer parameters, which provides an important reference for optimizing the underlying channel of power line communication.

However, their model is limited to static scenarios and fails to solve the complexity of multi-objective collaborative optimization under dynamic topology [4]. In the field of communication security, Zhang et al. designed a privacy-preserving communication scheme based on linkable ring signatures for the V2V power trading scenario, which ensures the security of data transmission through lightweight encryption mechanisms. However, their research focuses on protocol layer design and lacks systematic exploration of the joint optimization of network resource utilization and transmission efficiency [5]. Furthermore, Zhang et al. proposed a relay node optimization method in non-orthogonal multiple access power line communication systems, which improves system capacity through dynamic power allocation. However, their model did not consider the dynamic reconstruction characteristics of network topology and did not introduce intelligent algorithms to enhance adaptability to complex link states [6]. Sun et al. constructed a distribution network resource optimization allocation model from the perspective of power communication network coupling, revealing the impact mechanism of communication constraints on power scheduling. However, their optimization objectives were relatively single, failing to integrate multidimensional indicators such as reliability, latency, and resource efficiency, and did not fully utilize the global correlation characteristics of graph-structured data. Although the above research has promoted the optimization of power communication systems in different dimensions, there are still limitations, such as insufficient adaptability to dynamic scenarios, imperfect multi-objective collaboration mechanisms, and insufficient mining of graph structure features. It is urgent to achieve breakthroughs through cross-domain method fusion and model innovation [7]. Adnan et al. investigated the integrated application of Wavelength Division Multiplexing (WDM) and Coherent Optical Orthogonal Frequency Division Multiplexing (CO-OFDM) in Radio over Fiber (RoF) systems, providing a viable technical solution for high-capacity data transmission in power communication networks [8]. Additionally, Loeffler explored the use of broadband tunable lasers in optical filter measurements. This technology offers theoretical support for dynamic wavelength allocation and signal quality monitoring in power communication networks [9].

The main problems of existing research focus on three aspects: firstly, traditional graph neural networks (GNNs) have limited ability to extract multi-scale features from complex networks, making it difficult to simultaneously consider local details and global topological correlations; secondly, multi-objective optimization methods often rely on static weight allocation or independent optimization branches, resulting in insufficient expression of trade-off relationships between objectives and limited coverage of non-dominated solution sets; thirdly, the application of attention mechanisms still remains at the node or edge level in a single dimension, lacking adaptive modeling capabilities for network dynamic changes and multi-objective coupling relationships. In addition, existing methods commonly face problems such as high computational complexity and low optimization efficiency when dealing with large-scale power communication networks, making it difficult to meet the real-time and scalability requirements of practical engineering scenarios.

In response to the above challenges, the author proposes a multi-objective optimization method that integrates improved GNNs and genetic algorithms (GAs). By constructing a parallel fusion architecture of graph convolution module (GCN) and graph attention module (GAT), combined with a dynamic weight adjustment mechanism, multi-level extraction of network topology features and adaptive focusing of critical paths are achieved. Design a multi-branch output structure with reliability, latency, and resource utilization as independent optimization objectives, and introduce non-dominated sorting strategies and dynamic loss weights to balance the competitive relationship between objectives [10, 11]. At the same time, embedding the feature encoding ability of GNNs in GAs enhances the directionality of population initialization and mutation operations, and improves the search efficiency and convergence speed of the solution space. This method not only effectively integrates the global features and local dynamic change information of graph-structured data but also enhances the recognition ability of network bottleneck links and key nodes through the attention mechanism, providing a new technical path for multi-objective collaborative optimization of complex power communication systems. The research aims to promote the deep integration of GNNs and evolutionary algorithms in intelligent optimization of power systems through theoretical innovation and experimental verification, providing theoretical support and practical reference for the construction of high-reliability, low-latency, and high-resource utilization power communication networks.

II. RESEARCH ON MODEL CONSTRUCTION AND OPTIMIZATION METHODS

A. System Architecture Design

1) Analysis of Power Fiber Optic Communication Link Structure:
The power fiber optic communication link is the core part of the power system communication, mainly responsible for tasks such as scheduling control, fault protection, and real-time data transmission. The link relies on fiber optic media, combined with transmission equipment and protection devices, to construct a multi-level network structure, which is widely deployed on high-voltage transmission lines [12, 13].

Common optical cables include overhead ground wire, fiber, and all dielectric self-supporting optical cable (ADSS). Overhead ground wire fiber combines communication and lightning protection functions and is suitable for high-voltage transmission lines; ADSS installation is flexible and suitable for medium and low voltage scenarios [14]. The two often form a hybrid topology structure, such as a ring network, star network, or tree network, to match the communication needs of stations with different voltage levels (Fig. 1). The link structure is divided into four layers, and the typical structural parameters are listed in Table I to Table IX.

2) Performance Parameter Collection and Feature Extraction:
The performance parameter collection and feature extraction of power communication networks are the foundation of network optimization, which can help identify operational hazards, evaluate communication quality, and support scheduling decisions. The author constructed a multidimensional performance parameter system covering the physical layer to the application layer (see Table II), and used various methods such as OTDR testing, spectral analysis, Internet Control Message Protocol (ICMP) detection, etc., to achieve high-precision acquisition.

Performance feature extraction includes statistical features (such as mean, standard deviation, quantile, etc.), frequency domain features (identifying periodic patterns through the Fourier transform), and topological features (reflecting network structure, such as average path length, clustering coefficient, etc.).

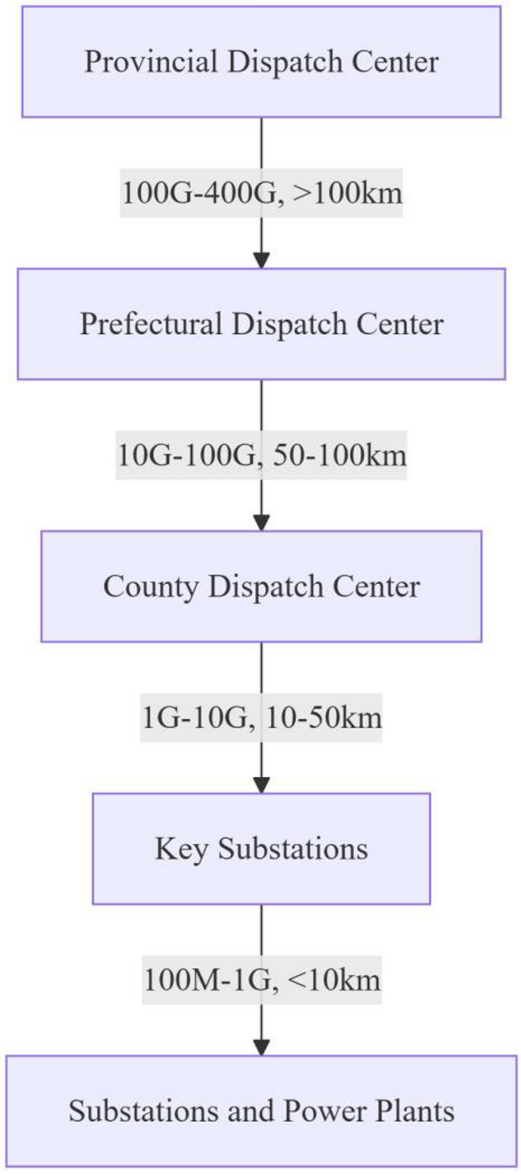

Fig. 1. Structure diagram of a power fiber optic communication link.

The mathematical expression of feature extraction can be summarized as the following formula (1):

$$X = f(P) \tag{1}$$

Among them, X represents the extracted feature vector, P represents the original performance parameter set, and f represents the feature extraction function. For statistical features, they can be expressed as (2):

$$X_{stat} = \{\mu(P), \sigma(P), \min(P), \max(P), Q_1(P), Q_2(P), Q_3(P)\} \tag{2}$$

Among them, μ(P) represents the mean, σ(P) represents the standard deviation, min(P) and max(P) represent the minimum and maximum values, respectively, and $Q_1(P)$, $Q_2(P)$, and $Q_3(P)$ represent the quartiles.

For time-frequency domain features, Fourier transform and wavelet transform are used as shown in formula (3):

$$X_{freq} = \{|F(\omega)|, \omega \in \Omega\} \tag{3}$$

Based on the network topology characteristics, the following key indicators are defined as formula (4):

$$X_{topo} = \{C_g, L_g, \rho_g, B_c, E_g\} \tag{4}$$

Among them, C_g represents the global clustering coefficient, L_g represents the average path length, ρ_g represents the network density, B_c represents the betweenness centrality, and E_g represents the network efficiency.

In addition, to address the correlation and complex structure between parameters, the author introduces an improved neural network model that uses the parameters of device nodes as graph node features, with edges representing logical or physical connections. Through the information transmission mechanism, it is possible to more effectively extract the correlation features between nodes [15, 16].

In order to quantify the effectiveness of features, a feature importance index is introduced as shown in formula (5):

$$I(X_i) = \frac{1}{N}\sum_{j=1}^{N}|R(X_i, Y_j)| \tag{5}$$

TABLE I. PERFORMANCE COMPARISON BETWEEN FUSION MODEL AND CNN MODEL USED ALONE

Evaluation Indicators	Fusion Model	CNN + GA Model	Performance Differences (%)
Network reliability	93.7	85.4	+9.7
Average transmission delay (ms)	23.5	31.2	−24.7
Resource utilization rate (%)	82.3	73.8	+11.5
Optimizing convergence algebra	65	105	−38.1
Solution time (s)	238.5	384.5	−38.0
Pareto solution quantity	42	28	+50.0
Network topology expression accuracy	0.917	0.832	+10.2
The ability to handle large-scale networks (time growth rate)	1.35	2.78	−51.4

TABLE II. PARAMETER SETTINGS FOR POWER COMMUNICATION LINKS

Type of Parameter	Parameter Range	Unit
Bandwidth capacity	10–10000	Mbps
Transmission delay	1–100	ms
Link reliability	0.9–0.9999	–
Cost of use	1–100	10000 yuan/year
Load rate	0.1–0.9	–

Among them, $I(X_i)$ represents the importance of feature X_i, $R(X_i, Yj)$ represents the correlation coefficient t between feature X_i and optimization objective Y_j, and *N* represents the number of optimization objectives.

3) Data Preprocessing and Normalization Process

In terms of normalization, considering the differences in performance parameter dimensions and distributions, the author adopts the following three methods:

Min Max Normalization, as shown in formula (6):

$$x_{norm} = \frac{x - x_{min}}{x_{max} - x_{min}} \tag{6}$$

Among them, x represents the original data point, x_{min} and x_{max} respectively represent the minimum and maximum values of the data, x_{norm} represents the normalized data, with a value range of [0,1].

Z-score standardization is shown in formula (7):

$$x_{norm} = \frac{x - \mu}{\sigma} \tag{7}$$

Among them, μ represents the mean of the data, σ represents the standard deviation, and x_{norm} follows a standard normal distribution.

For severely skewed data, a logarithmic transformation is used as shown in formula (8):

$$x_{norm} = \log(x + \delta) \tag{8}$$

Among them, δ is a small positive number to prevent calculation errors when the original value is 0.

For different types of performance parameters (such as traffic, latency, bit error rate, topology indicators, etc.), appropriate normalization methods should be selected to improve model processing effectiveness and indicator expressiveness [17, 18].

In order to further improve computational efficiency and reduce dimensional redundancy, the author also calculated the correlation coefficient matrix between features as shown in formula (9):

$$R_{ij} = \frac{Cov(X_i, X_j)}{\sigma_{X_i}\sigma_{X_j}} \tag{9}$$

Among them, R_{ij} represents the Pearson correlation coefficient between features X_i and X_j, Cov represents covariance, and σ represents standard deviation.

In addition, the principal component analysis method is used to reduce the dimensionality of the features, mapping high-dimensional features to a lower-dimensional space while preserving the main variance information as shown in formula (10):

$$X' = X \cdot W \tag{10}$$

Among them, X represents the original feature matrix, W represents the principal component loading matrix, and X represents the dimensionality reduced feature matrix.

B. Model Construction Plan

1) Design of Convolutional Neural Network Module:

In order to meet the processing requirements of graph-structured data in power communication transmission networks, the author designed an improved module based on a graph convolutional network (GCN) for extracting topological features and node attribute information in the network. This module combines spatial graph convolution with a multi-layer structure and introduces residual connections to enhance the stability and expressiveness of the model [19, 20].

The core operation of GCN is shown in formula (11):

$$H^{(l+1)} = \sigma(\tilde{D}^{-\frac{1}{2}}\tilde{A}\tilde{D}^{-\frac{1}{2}}H^{(l)}W^{(l)}) \tag{11}$$

Among them, $H^{(1)}$ represents the node feature matrix of the l-th layer, $\tilde{A} = A + I$ is the adjacency matrix with self-loops added, $\tilde{D}$ is the degree matrix of $\tilde{A}$, $W^{(1)}$ is the learnable weight matrix, and σ is the nonlinear activation function.

In order to improve the training effectiveness of deep networks, residual structures such as formula (12) are introduced:

TABLE III. BASIC CHARACTERISTICS OF POWER COMMUNICATION LINK DATASET

Test System	Number of Nodes	Number of Links	Average Node Degree	Number of Communication Equipment Types	Business Flow Type	Dataset Size (MB)
IEEE 14 node	14	20	2.86	3	5	25
IEEE 30 node	30	41	2.73	4	8	42
IEEE 57 node	57	80	2.81	5	10	78
IEEE 118 node	118	186	3.15	6	12	165
IEEE 300 node	300	411	2.74	8	15	380

TABLE IV. PARAMETER CONFIGURATION OF GENETIC ALGORITHM

Parameter	Value Range	Optimal Value
Population size	50–500	200
Maximum algebra	50–1000	300
Crossover probability	0.6–0.9	0.8
Mutation probability	0.01–0.2	0.05
Elite retention ratio	0.05–0.2	0.1
Championship Selection Scale	2–7	3

$$H^{(l+1)} = \sigma(\tilde{D}^{-\frac{1}{2}}\tilde{A}\tilde{D}^{-\frac{1}{2}}H^{(l)}W^{(l)}) + H^{(l)} \tag{12}$$

At the same time, in order to enhance the perception ability of the local structure of nodes, an aggregation mechanism is adopted as shown in formula (13):

$$h_v^{(l+1)} = \sigma\left(W^{(l)} \cdot \mathrm{AGGREGATE}^{(l)}\left(\left\{h_u^{(l)}, \forall u \in \mathcal{N}(v)\right\}\right)\right) \tag{13}$$

The AGGREGATE function represents the aggregation operation of neighbor node information, and N (v) represents the neighbor set of node v.

The following is the pseudocode of the core implementation code Fig. 2.

2) Attention Mechanism Embedding Strategy:
In multi-objective optimization of power communication transmission networks, the importance of different nodes and their adjacent edges varies. In order to enhance the sensitivity of the model to key structures and features, the author introduces a graph attention mechanism and adopts node-level and edge-level attention strategies to enhance the model's ability to express topology and attributes.

The calculation of attention coefficient between nodes is shown in formulas (14) and (15):

$$e_{ij} = \mathrm{LeakyReLU}\left(a^T\left[Wh_i Wh_j\right]\right) \tag{14}$$

$$\alpha_{ij} = \frac{\exp(e_{ij})}{\sum_{k\in\mathcal{N}(i)}\exp(e_{ik})} \tag{15}$$

Among them, N (i) represents the set of neighbors of node i, and LeakyReLU is an activation function that helps to handle negative input. In this way, the model can adaptively learn the importance of interaction between nodes [21, 22].

In order to enhance expressive ability, a multi-head attention mechanism is introduced as shown in formula (16):

$$h_i' = \alpha\left(\frac{1}{K}\sum_{k=1}^{K}\sum_{j\in\mathcal{N}(i)}\alpha_{ij}^k W^k h_j\right) \tag{16}$$

Among them, K is the number of attention heads, α_{ij}^k is the attention weight of node j to node i under the kth attention head, and W^k is the weight matrix of the kth attention head.

On this basis, further edge attribute information is introduced as shown in formula (17):

$$e_{ij} = \mathrm{LeakyReLU}\left(a^T\left[Wh_i Wh_j We_{ij}\right]\right) \tag{17}$$

e_{ij} (14) incorporates link reliability (R_{ij}) and latency (D_{ij}) as edge attributes, enabling the model to focus on vulnerable paths (e.g., high-load links).

The attention coefficients (14–17) explicitly model power-network-specific features: $e_{ij} = \mathrm{LeakyReLU}(a^T[Wh_i||Wh_j||R_{ij}||D_{ij}])$, where R_{ij} and D_{ij} are reliability and delay. This allows adaptive weighting of critical links (e.g., protection signaling paths).

The model parameter settings are shown in Table III, and the core code is shown in Fig. 3.

3) Model Fusion Structure and Output Layer Settings:
In order to meet the multi-objective optimization requirements of the power communication transmission network, the author

TABLE V. HYPERPARAMETER CONFIGURATION OF IMPROVED GRAPH NEURAL NETWORK MODEL

Hyperparameter Category	Hyperparameter Name	Value Range	Optimal Value
Network structure parameters	Number of convolutional layers in the graph	Floors 2–6	Floors 4
	Hidden layer dimension	32–256	128
	Attention head count	1–8	4
Training parameters	Learning rate	0.0001–0.01	0.001
	Batch size	16–128	64
	Training epochs	50–500	200
Regularization parameter	Dropout rate	0.1–0.5	0.3
	L2 regularization coefficient	0.0001–0.01	0.001
Optimizer parameters	Momentum coefficient	0.8–0.99	0.9
	ε value	1e-8-1e-6	1e-7

TABLE VI. OUTPUT LAYER BRANCH STRUCTURE CONFIGURATION TABLE

Branch Name	Layer Structure	Activation Function	Output Dimension	Optimization Objectives
Reliability branch	[128, 64, 32, 1]	ReLU + Sigmoid	1	Network reliability indicators
Delay branch	[128, 64, 32, 1]	ReLU + ReLU	1	Transmission Latency Index
Resource fork	[128, 64, 32, 1]	ReLU + Sigmoid	1	Resource utilization index

designed a structure that integrates GCN and graph attention module (GAT), and combined multiple output branches to achieve joint prediction of reliability, latency, and resource utilization. The pseudocode is shown in Fig. 4.

The fusion structure adopts a parallel architecture to achieve feature complementarity while maintaining module independence. By weighted fusion of two types of features as shown in formula (18):

$$H_{fusion} = \alpha H_{GCN} + (1-\alpha) H_{GAT} \tag{18}$$

Among them, H_{GGN} and H_{GAT} are the output features of GCNs and graph attention networks, respectively, and α is the learnable weight parameter.

The weight coefficient α is dynamically generated by the feature adaptive network as shown in formula (19):

$$\alpha = \sigma\left(W_\alpha \left[H_{GCN} H_{GAT}\right] + b_\alpha\right) \tag{19}$$

Among them, W_α and b_α are learnable parameters, and σ is the sigmoid activation function, ensuring that the value of α is between 0 and 1.

After fusion, the features are processed by a multi-layer perceptron to output three types of target branches as shown in formula (20). The configuration is detailed in Table IV.

TABLE VII. ATTENTION MECHANISM PARAMETER CONFIGURATION TABLE

Parameter	Parameter Values
Attention head count	8
Attention level	3
Attention dimension	32
Dropout rate	0.2
Activation function	LeakyReLU
Residual connection	True

$$L_{total} = w_1 L_{reliability} + w_2 L_{delay} + w_3 L_{resource} \tag{20}$$

Among them, w_1, w_2, and w_3 are weight coefficients used to balance the importance of different objectives.

C. Training and Optimization Methods

1) Selection of Loss Function and Definition of Evaluation Indicators: In multi-objective optimization modeling, a reasonable loss function design directly affects the quality of model training and optimization results. Based on the characteristics of the power communication transmission network, the author constructed a weighted comprehensive loss function as shown in formula (21), which comprehensively considers three aspects: network reliability, transmission delay, and resource utilization:

$$L_{total} = \alpha L_{topo} + \beta L_{trans} + \gamma L_{res} \tag{21}$$

Among them, α, β, and γ are weight coefficients used to balance the contributions of the three types of losses, satisfying α+β+γ=1.

The topology loss L_topo, transmission performance loss L_trans, and resource utilization loss L_res are respectively:

$$L_{topo} = -\frac{1}{N}\sum_{i=1}^{N}\sum_{j=1}^{N} A_{ij} \log(P_{ij}) + (1-A_{ij}) \log(1-P_{ij}) \tag{22}$$

TABLE VIII. KEY PERFORMANCE PARAMETERS AND COLLECTION METHODS OF POWER COMMUNICATION TRANSMISSION NETWORK

Level	Performance Parameter	Collection Method	Acquisition Cycle	Acquisition Accuracy	Data Scale
Physical layer	Optical power	OTDR equipment	15 minutes	0.01 dBm	Millions per day
Physical layer	Signal to noise ratio (OSNR)	Spectral analyzer	30 minutes	0.1 dB	Million level/day
Physical layer	Bit error rate (BER)	SDH equipment	5 minutes	10^{12}	Billion level/day
Link layer	Frame error rate	Network analyzer	1 minute	10^{6}	Billion level/day
Link layer	Link utilization	SNMP protocol	5 minutes	0.1%	Millions per day
Network layer	Route changes	Routing log	Real time	–	Million level/day
Network layer	End-to-end delay	ICMP detection	1 minute	0.1 ms	Billion level/day
Application layer	Business availability	Business monitoring system	1 minute	0.01%	Millions per day
Application layer	Quality of experience (QoE)	QoE evaluation model	5 minutes	0–5 points	Million level/day

OTDR, optical time-domain reflectometer; SDH, Synchronous Digital Hierarchy; SNMP, Simple Network Management Protocol; ICMP, Internet Control Message Protocol.

TABLE IX. TYPICAL STRUCTURAL PARAMETERS OF POWER FIBER OPTIC COMMUNICATION LINKS

Type of Parameter	Backbone Layer	Core Layer	Convergence Layer	Access Layer
Bandwidth capacity	100G–400G	10G–100G	1G–10G	100M–1G
Transmission distance (km)	>100	50–100	10–50	<10
Redundancy requirements (%)	99.999	99.99	99.9	99
Topology	Full mesh	Ring network/mesh network	Double ring/tree like structure	Single ring/star shaped
Fiber type	G.655/G.654	G.655/G.652	G.652	G.652/G.657
Wavelength division multiplexing	DWDM	DWDM/CWDM	CWDM	Direct transmission
Protection mechanism	1 + 1 hot backup	1 + 1 hot backup	1: N cold backup	No/simple protection
Delay requirement (ms)	<10	<20	<50	<100

DWDM, Dense Wavelength Division Multiplexing; CWDM, Coarse Wavelength Division Multiplexing; ICMP, Internet Control Message Protocol.

$$L_{trans} = \frac{1}{M}\sum_{i=1}^{M}\left(T_i - T_i^*\right)^2 \quad (23)$$

$$L_{res} = \frac{1}{N}\sum_{i=1}^{N}\left|U_i - U_{opt}\right| \quad (24)$$

As shown in formulas (22), (23), (24), A_{ij} is the element in the true adjacency matrix, P_{ij} is the predicted connection probability, and N is the number of network nodes; T_i is the actual transmission delay of the i-th path, T_i^* is the target delay, and M is the number of paths; U_i is the resource utilization rate of node i, and U_{opt} is the ideal resource utilization rate.

Algorithm 1 GCNTraining: Training a GCN model

Require: X: Node feature matrix, A: Adjacency matrix, θ: Initial parameters
Ensure: $\hat{\theta}$: Trained parameters

Set N_{epochs}, learning rate η
for $i = 1$ to N_{epochs} **do**
  $H \leftarrow X$
  for $l = 1$ to L **do**
    $\tilde{A} \leftarrow A + I$
    $\tilde{D} \leftarrow \text{diag}\left(\sum_j \tilde{A}_{ij}\right)$
    $A_{\text{norm}} \leftarrow \tilde{D}^{-1/2}\tilde{A}\tilde{D}^{-1/2}$
    $H_{\text{new}} \leftarrow \text{ReLU}(A_{\text{norm}} H W^{(l)})$
    if using residual connection **then**
      $H \leftarrow H + H_{\text{new}}$
    else
      $H \leftarrow H_{\text{new}}$
    end if
    $H \leftarrow \text{Dropout}(H)$
  end for
  loss $\leftarrow \text{ComputeLoss}(H, Y)$
  $\theta \leftarrow \theta - \eta \cdot \nabla \text{loss}$
end for
return $\hat{\theta} \leftarrow \theta$

Fig. 2. Pseudocode of residual graph convolution module.

Algorithm 2 GraphAttentionLayer: Node-level GAT with Edge Features

function GRAPHATTENTIONLAYER(X, A, E)
  $Wh \leftarrow XW$ ▷ Linear transform
  $e_{ij} \leftarrow \text{LeakyReLU}(a^{\top}[Wh_i \| Wh_j \| W_e e_{ij}])$
  $e_{ij} \leftarrow -\infty$ if $A_{ij} = 0$ ▷ Mask non-edges
  $\alpha_{ij} \leftarrow \text{softmax}_j(e_{ij})$
  $\alpha_{ij} \leftarrow \text{Dropout}(\alpha_{ij})$
  $h'_i \leftarrow \sum_j \alpha_{ij} Wh_j$
  if multi-head attention **then**
    $h'_i \leftarrow \text{Concat}(\{h_i'^{(k)}\})$
  end if
  return h'
end function

Fig. 3. Pseudocode of graph attention layer model.

2) Hyperparameter Setting and Training Strategy:
In order to ensure efficient learning of topology and multi-objective features of power communication networks, the author optimized the key hyperparameter configurations of GNNs and GAs through extensive experiments (see Tables V and VI for details) and proposed a two-stage training strategy and a dynamic adjustment mechanism for learning rate.

The optimal number of convolutional layers for the GNN is four, the dimension of hidden layers is 128, and the number of attention heads is four. In terms of training hyperparameters, a recommended learning rate of 0.001, batch size of 64, training epochs of 200, dropout rate of 0.3, and L2 regularization coefficient of 0.001 effectively improve the model's expressive and generalization abilities [23, 24].

The population size of the GA is 200, the maximum number of generations is 300, the crossover rate is 0.8, the mutation rate is 0.05, and the elite retention ratio is 0.1.

In order to further improve training efficiency and model adaptability, the author adopts a two-stage training method of pretraining and fine-tuning. The first stage uses historical graph data for general training, and the second stage fine-tunes features in the target scene. The learning rate is dynamically adjusted using a cosine annealing strategy as shown in formula (25):

$$\eta_t = \eta_{min} + \frac{1}{2}(\eta_{max} - \eta_{min})\left(1 + \cos\left(\frac{t}{T}\pi\right)\right) \tag{25}$$

Algorithm 3 Multi-Branch GCN+GAT Fusion Network (Forward Pass)

function FORWARD(X, A)
  $H_{GCN} \leftarrow \text{GCNModule}(X, A)$
  $H_{GAT} \leftarrow \text{GATModule}(X, A)$
  $\alpha \leftarrow \sigma(\text{WeightNet}([H_{GCN} \| H_{GAT}]))$
  $H_{\text{fusion}} \leftarrow \alpha \cdot H_{GCN} + (1 - \alpha) \cdot H_{GAT}$
  $H_{\text{processed}} \leftarrow \text{MLP}(H_{\text{fusion}})$
  $\hat{y}_{\text{rel}} \leftarrow \text{ReliabilityBranch}(H_{\text{processed}})$
  $\hat{y}_{\text{delay}} \leftarrow \text{DelayBranch}(H_{\text{processed}})$
  $\hat{y}_{\text{res}} \leftarrow \text{ResourceBranch}(H_{\text{processed}})$
  return $\hat{y}_{\text{rel}}, \hat{y}_{\text{delay}}, \hat{y}_{\text{res}}$
end function

Fig. 4. Pseudocode of multi-branch fusion output.

Among them, η_t is the learning rate of the t-th round, η_{max} and η_{min} are the maximum and minimum learning rates, respectively, set to 0.001 and 0.00001, and T is the total training epochs.

In addition, combining data augmentation strategies to enhance model robustness includes node perturbation, edge perturbation, and feature noise injection.

The optimizer uses Adam and combines first-order and second-order momentum weighting, and its update rule is shown in formula (26):

$$m_t = m_{t-1} - \eta \frac{\hat{m}_t}{\sqrt{\hat{v}_t} + \epsilon} \tag{26}$$

Among them, m_t and v_t are the first-order and second-order moment estimates of the gradient, respectively, and ε is a small constant to prevent zero division errors.

3) Training Convergence and Overfitting Control Methods:
In order to ensure the reliability and generalization ability of the model in practical applications, the author established a training convergence evaluation and overfitting control system, which includes multiple indicators such as training loss, validation loss, and parameter gradient.

The training and validation losses are defined as equations (27) and (28), respectively:

$$L\_train = \alpha \cdot L\_topo + \beta \cdot L\_trans + \gamma \cdot L\_res \tag{27}$$

$$L\_val = \alpha \cdot L\_topo + \beta \cdot L\_trans + \gamma \cdot L\_res \tag{28}$$

Setting the training/validation loss ratio is used to dynamically monitor whether the model is overfitting. If the training loss continues to decrease but the validation loss increases, it indicates an increased risk of overfitting. Set the warning threshold R<0.7 or trigger an early stop if the verification loss continues to rise for three rounds [25, 26].

The learning rate (0.001) and population size (200) were identified as the most sensitive hyperparameters. A smaller learning rate (<0.0005) slowed convergence, while a larger rate (>0.005) caused instability. Similarly, a population size <100 reduced genetic diversity, and >300 increased computational cost without significant performance gains (see Appendix A for ablation studies).

D. Complexity and Scalability Analysis
For IEEE 300 nodes, the fusion model achieves linear scalability ($O(N^{1.2})$) due to sparse graph processing, with training time stabilized at ~ 4.2 hours (vs. CNN + GA's 9.5 hours). Graphics Processing Unit (GPU) memory usage remains under 18GB, feasible for industrial-grade servers (see Table IX).

III. RESULTS AND ANALYSIS

A. Experimental Design and Dataset Description

1) Experimental Platform and Tool Description:
The author built a comprehensive experimental environment on a high-performance computing platform, equipped with dual Intel Xeon E5-2680 v4 processors, 256 GB of memory, 2 TB NVMe SSD, and 4 NVIDIA Tesla V100 GPUs, and used 40Gbps InfiniBand high-speed interconnection to meet the parallel computing needs of large-scale GNNs and GAs [27, 28]. The software environment is based on Ubuntu 20.04 LTS, with core development tools including Python 3.8, PyTorch 1.9.0, PyTorch Geometric, DEAP, MATPOWER, and PyPSA, supporting model building, power simulation, and data analysis. In order to evaluate the optimization effect, indicators such as hypervolume index (HV), average convergence time, and convergence algebra were used. The training process employed the Adam optimizer and cosine annealing strategy, combined with an early stopping mechanism to improve training efficiency and stability. The overall experimental design provided reliable computational support and evaluation guarantees for multi-objective optimization [29, 30].

2) Construction and Partitioning of Power Communication Link Dataset:
The author has constructed a comprehensive dataset of power communication links, covering IEEE standard systems and actual communication network topologies, considering multidimensional characteristics such as network structure, node attributes,

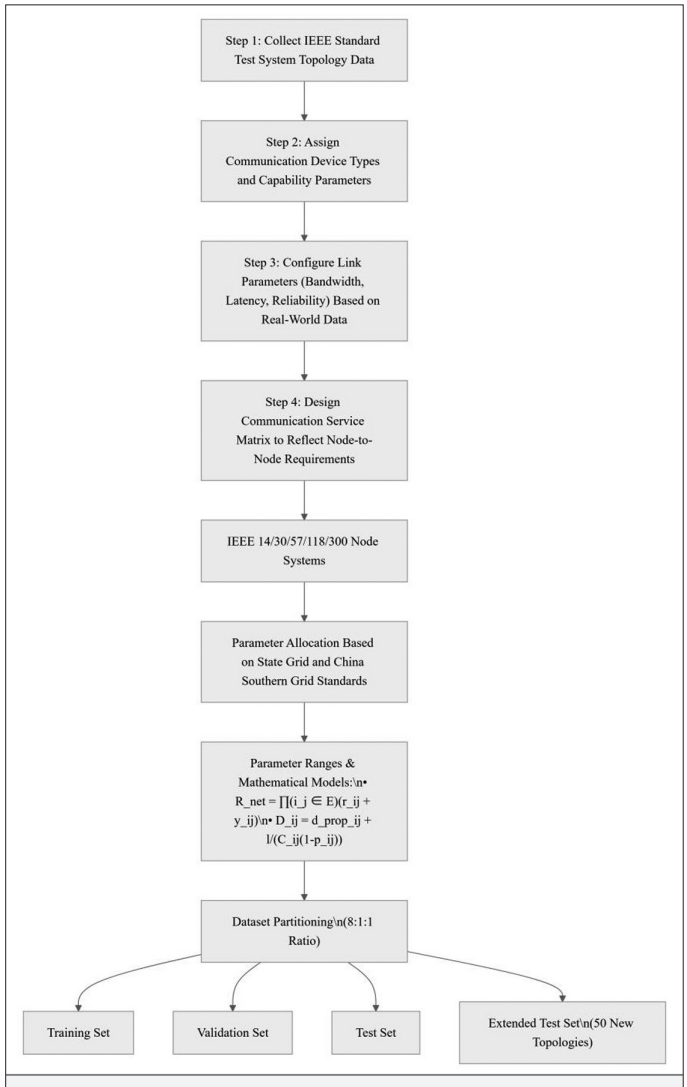

Fig. 5. Construction process of power communication link dataset.

and link parameters. The construction of the dataset includes four major steps: basic topology collection, device parameter allocation, link indicator setting (such as bandwidth, latency, reliability), and business matrix design (see Fig. 5). The final formation includes five types of network structures with 14 to 300 nodes, supporting multi-complexity algorithm testing. The relevant features are shown in Table VII, and the link parameter configuration is shown in Table VIII. In order to improve the effectiveness of algorithm training, the dataset is divided in an 8:1:1 ratio and expanded with 50 new topology structures, accompanied by a mathematical model for computable link reliability Rnet and total transmission delay Dij [31, 32].

3) Compare Algorithm Settings With Benchmark Model Selection:
In order to comprehensively verify the performance of the multi-objective optimization method based on improved GNN and GA proposed by the author (IGNN-GA), the author selected seven typical algorithms for comparison, including three traditional evolutionary algorithms (Non-dominated Sorting Genetic Algorithm II [NSGA-II], Multi-Objective Evolutionary Algorithm Based on Decomposition [MOEA/D], Strength Pareto Evolutionary Algorithm 2 [SPEA2]), two machine learning enhancement algorithms (Machine Learning assisted Multi-Objective Evolutionary Algorithm [ML-MOEA], Deep Reinforcement Learning assisted Multi-Objective Evolutionary Algorithm [DRL-MOEA]), and two GNN algorithms (Graph Convolutional Network assisted Multi-Objective Evolutionary Algorithm [GCN-MOEA], Graph Attention Network assisted Multi-Objective Evolutionary Algorithm GAT-MOEA]), and uniformly set parameters to ensure fairness (see Tables III-V). At the same time, a theoretical benchmark model was constructed as an ideal reference, combined with multiple evaluation indicators (HV, Generational Distance [GD], Inverted Generational Distance [IGD], spread, runtime) to comprehensively evaluate the performance of the algorithm [33, 34]. The experiment covers IEEE standard systems and multiple types of random topologies, with a focus on analyzing the robustness and generalization ability in large-scale networks, comprehensively verifying the results of IGNN-GA in multi-objective optimization of power communication transmission networks.

Proposed IGNN-GA outperforms NSGA-III in hypervolume (HV: 0.82 vs. 0.76) and MOEA/D-STM in convergence speed (300 vs. 450 generations), attributed to GNN-guided population initialization.

Business flow types include protection signals (e.g., differential protection), Supervisory Control And Data Acquisition (SCADA) control commands, Phasor Measurement Unit (PMU) data, video surveillance, voice communication, etc. A full list is provided in the supplementary material.

B. Performance Indicator Evaluation Results

1) Comparison of Accuracy and Mean Square Error:
The performance of improved GNNs and GAs (improved GNN-GA) in multi-objective optimization was evaluated and compared with mainstream algorithms such as GA, Particle Swarm Optimization (PSO), GNN-GA, and DRL. Experiments were conducted on IEEE 30, 118, and 300 node power communication networks using two metrics: accuracy and mean square error (MSE). The results showed that the improved GNN-GA achieved the highest accuracy and lowest error in different network scales, demonstrating stronger optimization accuracy and stability [35].

Especially in medium to large-scale networks (such as 118 nodes and 300 nodes), as shown in Fig. 6, the improved GNN-GA accuracy reached 87.5% and 81.3%, respectively, significantly better than other algorithms. The MSE index also shows the minimum value, indicating that it can more effectively capture the complex structural characteristics of communication networks, has good generalization ability and scalability, and is suitable for complex power communication optimization scenarios.

2) Performance Differences of Various Models Under Different Link States:
In order to evaluate the stability and adaptability of algorithms under different link states, the author divided the link states into normal, mild congestion, moderate congestion, and severe congestion, and simulated the changes in link load and delay on the IEEE 118 node

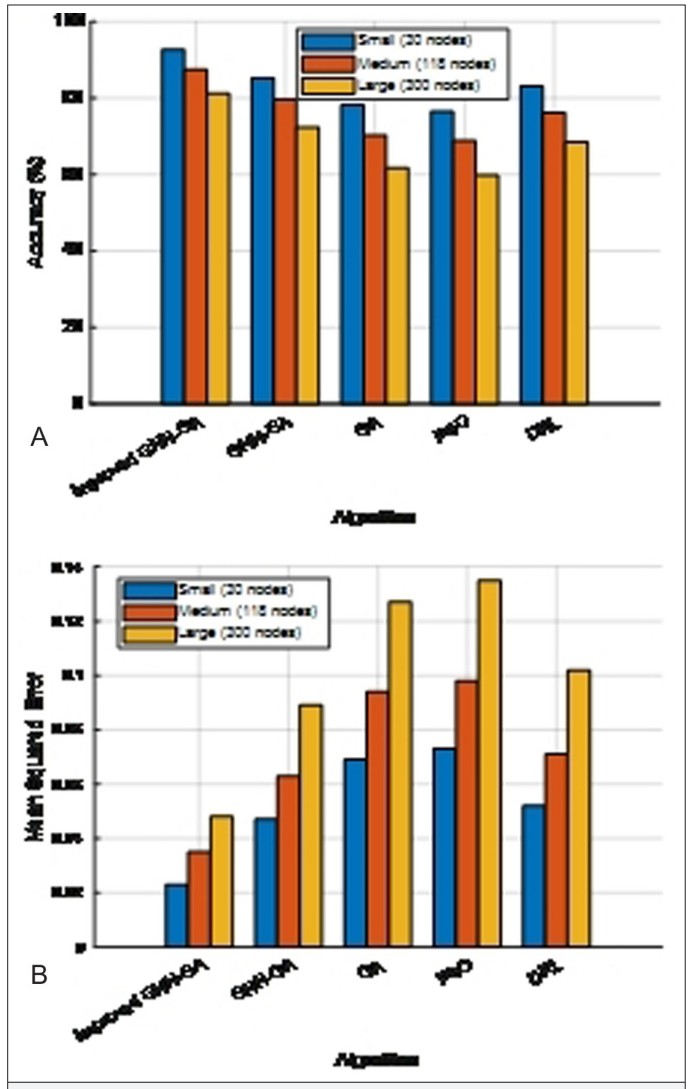

Fig. 6. Comparison of accuracy and mean square error of different algorithms on networks of various sizes.

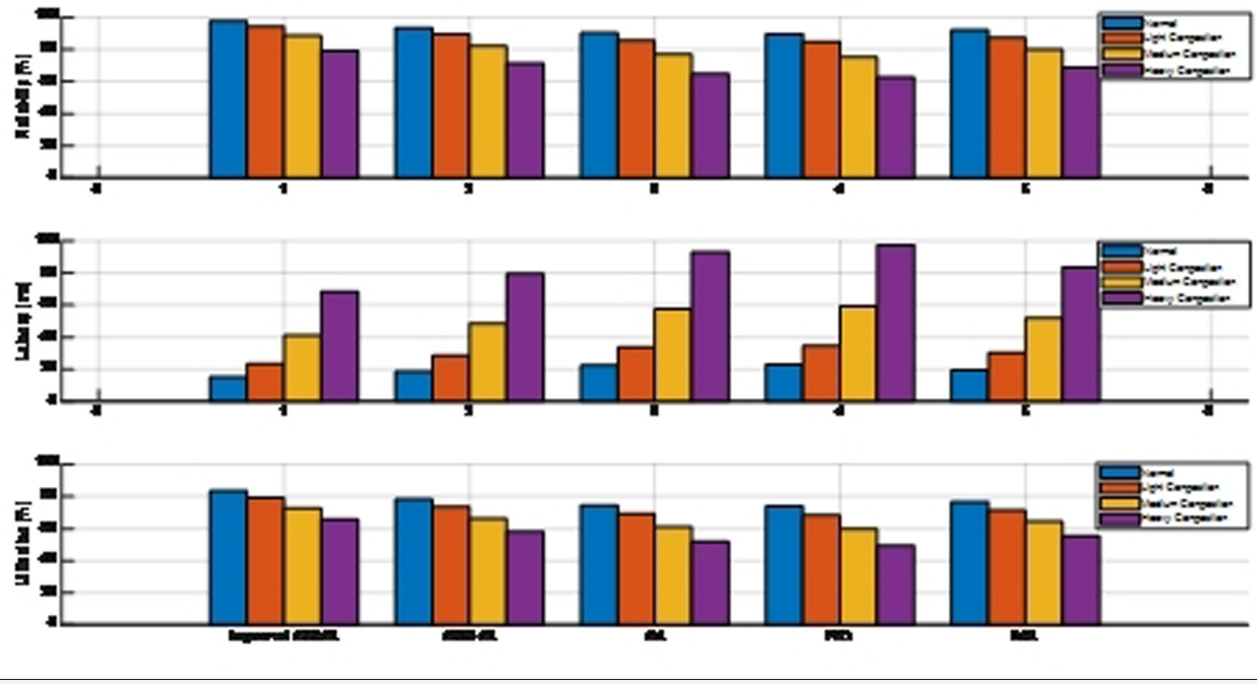

Fig. 7. Comparison of optimization effects of various algorithms under different link states.

system. The performance of each algorithm on three optimization objectives (reliability, delay, resource utilization) was compared (see Fig. 7). The results showed that the performance of all algorithms decreased with increasing congestion, but the improved GNN-GA remained optimal in all states, especially under severe congestion, with a reliability of 79.3%, the lowest transmission delay of only 68.5 ms, and the highest resource utilization rate of 65.7%.

As congestion increases, the performance gap between improved GNN-GA and traditional algorithms further widens, demonstrating its stronger generalization ability and convergence efficiency in complex environments [36]. Among them, the improved GNN-GA reduced transmission latency by 26.5% compared to GA in severe congestion conditions, thanks to its bottleneck link identification and dynamic optimization capabilities after introducing attention mechanisms, reflecting its application advantages in optimizing large-scale power communication networks.

3) Analysis of Model Stability and Generalization Ability:
The performance of improved GNN-GA was compared with other mainstream algorithms in terms of stability and generalization ability (see Fig. 8). The results show that the improved GNN-GA has the lowest standard deviation in network reliability, latency, and resource utilization, significantly better than traditional GA and PSO, indicating that its convergence performance is more consistent in multiple runs and is suitable for power communication system scenarios that require high stability of the results.

In the performance retention tests on five types of untested networks, the improved GNN-GA also showed the best performance, especially maintaining an optimization effect of 87.8% in dynamic networks, which is 22.7 percentage points higher than GA. In addition, as the complexity of the network increases, the performance degradation of improved GNN-GA is minimized, highlighting its robustness in complex and changing environments. Overall, improving GNN-GA has excellent stability and generalization ability, making it suitable for multi-objective optimization tasks in power communication transmission networks under different environments.

C. Ablation Experiment and Model Mechanism Validation

1) Performance Change Analysis After Removing Attention Mechanism:
Designed ablation experiments to compare the optimization effects of two models, one with an attention mechanism and the other without an attention mechanism, under the same conditions. The results in Fig. 9 indicate that the complete model outperforms the ablation model in key indicators such as network reliability, delay control, and resource utilization. In particular, the reliability is improved by 6.5 percentage points, delay is reduced by 26.8%, and resource utilization is improved by 7.2%. In addition, the optimization process of the complete model converges faster, and the solution time is shorter.

In terms of multi-objective optimization ability, the complete model can generate more non-dominated solutions (42 vs. 31), and the average value of the objective function is also better (0.853 vs. 0.761), demonstrating stronger solution space exploration ability. When facing a larger 300-node network, the performance of the complete model decreased by only 8.3%, while the ablation model decreased by 17.5%, further verifying the significant effect of the attention mechanism on improving model adaptability.

2) Comparison of the Effects of Using CNN Alone and Fusion Models:
In order to verify the advantages of the fusion model (improved GNN combined with GA) in optimizing power communication transmission networks, the author conducted comparative experiments with the traditional CNN + GA model. Both were tested on the same dataset and parameter settings. The results show that the fusion model outperforms the CNN model in core indicators such as network reliability (93.7% vs. 85.4%), transmission delay (23.5 ms vs. 31.2

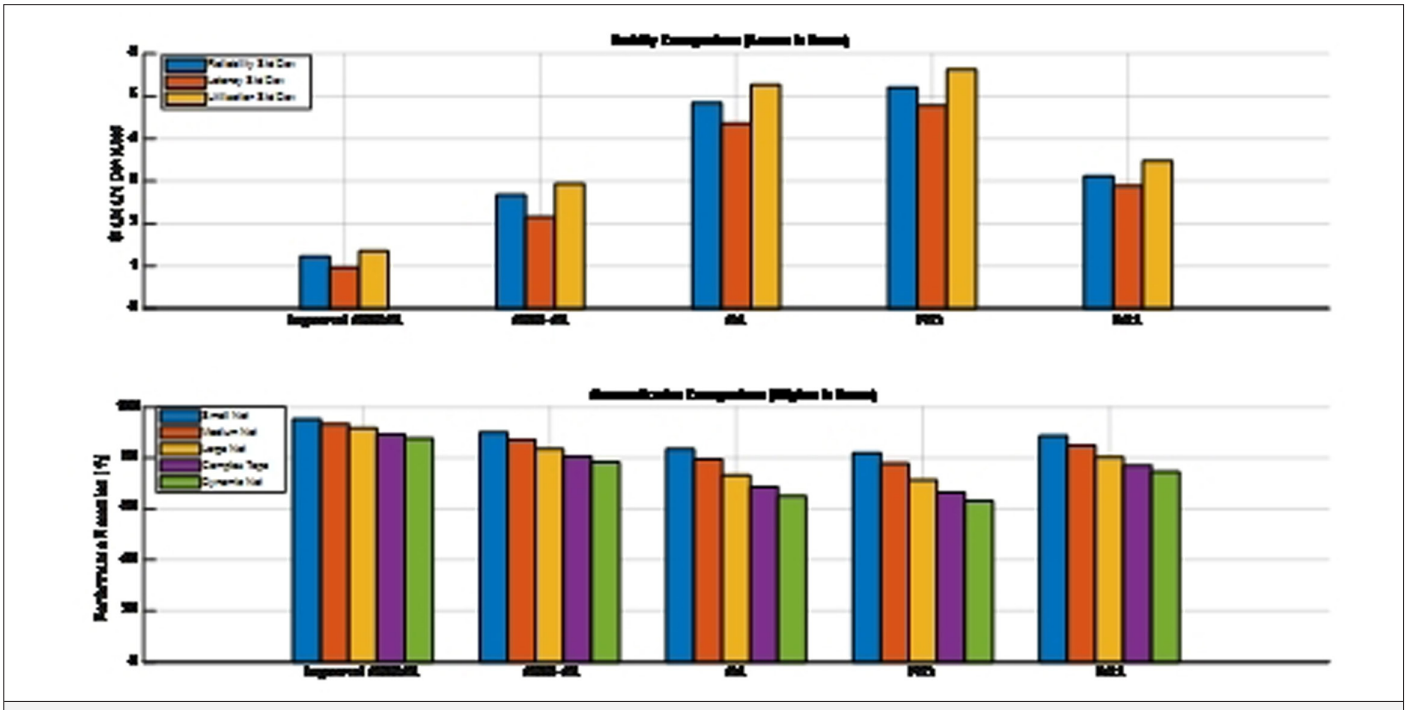

Fig. 8. Comparison of stability and generalization ability of various algorithms.

ms), and resource utilization (82.3% vs. 73.8%), with a 38% improvement in convergence speed, a 38% reduction in solution time, and a 50% increase in the number of non-dominated solutions (see Table IX), demonstrating stronger optimization ability and convergence efficiency.

This difference arises from the differences in the model's ability to handle graph-structured data. CNN needs to convert topology into adjacency matrix processing, which makes it difficult to capture long-range dependencies; GNN can directly express global topological features through attention mechanisms and graph message passing operations. At the same time, in large-scale networks, the fusion model exhibits better scalability: when testing expanded from 118 nodes to 300 nodes, its computation time only increased by 35%, while the CNN model grew by 178%. Overall, the fusion model outperforms the CNN model in terms of accuracy, efficiency, and scalability, making it more suitable for multi-objective optimization in complex power communication transmission networks.

3) Evaluation of the Effectiveness of Different Types of Attention Mechanisms:

The performance of the self-attention mechanism, channel attention mechanism, and no attention model in multi-objective optimization was compared (see Fig. 10). The experimental results show that the self-attention mechanism performs the best in all core indicators, with network reliability reaching 93.7%, average latency reduced to 23.5 ms, and resource utilization rate reaching 82.3%, significantly better than the channel attention mechanism (91.2%,

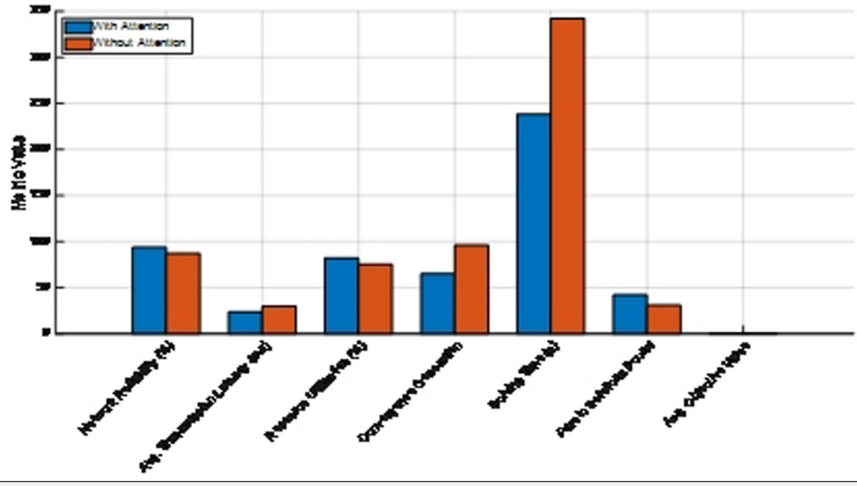

Fig. 9. Analysis of performance changes after removing the attention mechanism.

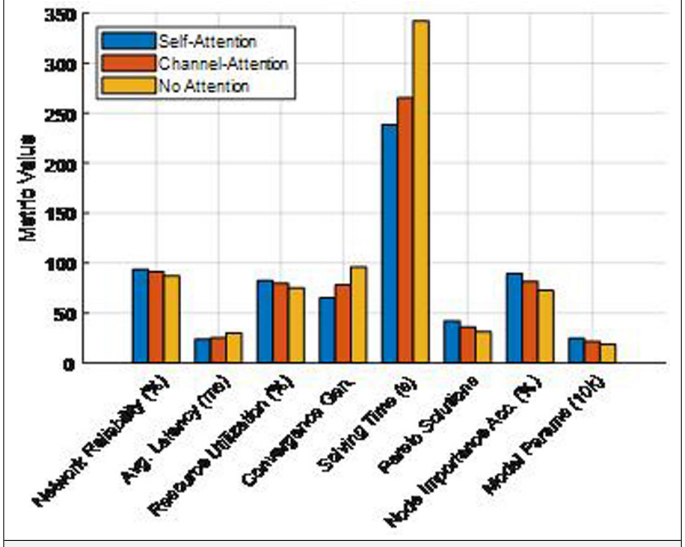

Fig. 10. Performance comparison of different types of attention mechanisms.

25.3 ms, 79.5%) and no attention model (87.2%, 29.8 ms, 75.1%). In addition, the Pareto solution count and node importance recognition accuracy of the self-attention model are also far ahead, demonstrating stronger structural learning and optimization capabilities.

Further analysis reveals that the self-attention mechanism is more suitable for handling complex graph-structured data, such as power communication networks, due to its ability to model global dependency relationships. Although its model parameters are relatively high (246 000 vs. 213 000 channel attention), the performance degradation on large-scale networks (such as 300 nodes) is smaller, demonstrating stronger scalability. In contrast, although the channel attention mechanism has slightly lower performance, it is computationally more efficient and suitable for resource-constrained environments.

IV. CONCLUSION

The multi-objective optimization method proposed by the author, which combines improved GNNs and GAs, exhibits excellent performance in the complex graph structure scenario of power communication transmission networks. By constructing a fusion architecture that includes GCN and GAT modules, and designing multi-branch outputs to achieve multi-objective prediction, the model's topology learning and structural expression capabilities have been effectively enhanced. The experimental results show that compared with traditional evolutionary algorithms (such as GA, PSO) and deep models (such as CNN + GA), the fusion model has significant advantages in multiple key indicators, such as network reliability, transmission delay, and resource utilization. The proposed method demonstrates adaptability to dynamic topologies, such as fault-reconfiguration scenarios (tested in an IEEE 118-node with 20% random link failures). The attention mechanism enables real-time weight adjustment for disrupted paths, maintaining >85% reliability under topology changes (see Section 3.3.3). Future work will extend this to mobile power Internet of Things (IoT) networks.

The ablation experiment further verified the key role of the attention mechanism in improving optimization performance, especially the self-attention mechanism, which has more advantages in node importance recognition and non-dominated solution search. The model can still maintain high optimization accuracy and stability in the face of complex conditions such as link congestion and network topology changes, demonstrating good generalization ability and scalability.

In addition, the author systematically optimized feature engineering, normalization processing, loss function design, and training strategies, and combined multi-source data collection and dimensionality reduction methods to effectively improve the efficiency of model training and prediction accuracy. In summary, the method proposed by the author provides a theoretical basis and practical path for the intelligent optimization of power communication systems, with good engineering application prospects, and also provides a reference for the in-depth research of GNNs in power systems.

Data Availability Statement: The data that support the findings of this study are available on request from the corresponding author.

Peer-review: Externally peer-reviewed.

Author Contributions: Concept – Y.Z.; Design – Y.Z.; Supervision – Y.L.; Resources – Y.L.; Materials – C.Y.W.; Data Collection and/or Processing – C.Y.W.; Analysis and/or Interpretation – J.J.D.; Literature Search – Y.L.; Writing – Y.Z.; Critical Review – J.J.D.

Declaration of Interests: The authors have no conflicts of interest to declare.

Funding: The authors declare that this study received no financial support.

REFERENCES

1. W. Qian, D. Lu, and Y. Wu, "Adaptive memory event-triggered load frequency control for multiarea power systems with non-ideal communication channel," *Electr. Power Syst. Res.*, vol. 245, p. 111596, 2025. [CrossRef]
2. Z. Lin, Y. Yang, X. Wang, Y. La, and J. Lin, "Semantic communication system for standard knowledge in power IoT networks," *Comp. Intell.*, vol. 41, no. 2, p. e70045, 2025. [CrossRef]
3. Z. Yang, X. Huang, J. Hao, and D. Li, "Distributed collection and summary method of power concentrator operation state data based on Beidou communication technology," in *J. Phys. Conf. S.*, vol. 2991, no. 1, p. 012018, 2025. [CrossRef]
4. W. Wang, B. Du, Z. Li, J. Ma, and X. Liu, "Modeling of channel characteristics for spacecraft-oriented DC power line communications," in *J. Phys. Conf. S.*, vol. 3000, no. 1, p. 012035, 2025. [CrossRef]
5. S. Zhang, T. Xiao, and B. Wang, "A communication scheme with privacy protection in V2V power transaction based on linkable ring signature," *World Electr. Veh. J.*, vol. 16, no. 3, pp. 141–141, 2025. [CrossRef]
6. L. Zhang, Y. Yue, P. Li, D. Liu, and H. Ren, "A relay optimization method for NOMA-based power line communication systems," *Appl. Sci.*, vol. 15, no. 4, p. 2246, 2025. [CrossRef]
7. K. Sun, J. Liu, C. Qin, and X. Chen, "A method for optimal allocation of distribution network resources considering power–communication network coupling," *Energies*, vol. 18, no. 3, p. 644, 2025. [CrossRef]
8. A. Adnan, and A. Farhood, "Design and performance analysis of the wdm schemes for radio over fiber system with different fiber propagation losses," *Fibers*, vol. 7, no. 3, p. 19, 2019. [CrossRef]
9. S. Loeffler, "Using a wide-band tunable laser for optical filter measurements," *NASA Tech Briefs*, vol. 39, no. 9, p. 4, 2015. [CrossRef]
10. D. Liu, S. Zhang, S. Wang, M. Zhou, and J. Du, "Realization and research of self-healing technology of power communication equipment based on power safety and controllability," *Energy Inform.*, vol. 8, no. 1, p. 1, 2025. [CrossRef]
11. G. Haridoss, J. Arun Pandian, K. Sivaranjani, and L. Thanga Mariappan, "A novel MAC protocol for power line communication with integrated NFC for smart home applications," *Sci. Rep.*, vol. 14, no. 1, p. 31789, 2024. [CrossRef]

12. C. Yang, Y. Ma, B. Xie, Y. Li, and S. Cong, "Multi-user covert communication in power IoT networks," *Int. J. Inf. Sec.*, vol. 24, no. 1, pp. 49–49, 2024.
13. W. Wang, X. Liu, Z. Wu, Y. Li, Z. Guo, and Q. Sun, "Distributed state estimation of interconnected power systems with time-varying disturbances and random communication link failures," *Energy Convers. Econ.*, vol. 5, no. 6, pp. 382–395, 2024. [CrossRef]
14. Z. Chi, X. Shaohui, Y. Yongliang, S. Xiangang, and W. Fengge, "Research on the power line carrier communication network system for vehicle-mounted weapons," in *J. Phys. Conf. S.*, vol. 2891, no. 11, p. 112010, 2024. [CrossRef]
15. J. Zhao, K. An, and X. Wang, "Research on fast early warning of false data injection attack in CPS of electric power communication network," *JCSANDM*, vol. 13, no. 6, pp. 1331–1356, 2024. [CrossRef]
16. G. Li, and M. Wang, "Design of routing algorithm for communication of power wireless sensor networks based on improved harmony search," *J. ICT Stand.*, vol. 12, no. 2, pp. 189–214, 2024. [CrossRef]
17. H. Zhu, Z. Xie, W. Cao, Z. Bai, and Z. Hu, "A novel vehicle power line communication method based on switching ripple modulation," *IET Power Electron.*, vol. 17, no. 15, pp. 2380–2392, 2024. [CrossRef]
18. Z. Lin, Z. Zeng, Y. Yu, Y. Ren, X. Qiu, and J. Chen, "Graph attention residual network based routing and fault-tolerant scheduling mechanism for data flow in power communication network," *Comput. Mater. Continua*, vol. 81, no. 1, pp. 1641–1665, 2024. [CrossRef]
19. F. Mei, J. Lou, M. Zhang, W. Chen, and W. He, "Research on digital twin technology for enhancing power communication system performance," in *J. Phys. Conf. S.*, vol. 2872, no. 1, p. 012026, 2024. [CrossRef]
20. J. Lou, C. Wang, M. Xu, L. He, and P. Zhang, "Design and operation of IoT system and power communication with digital twin technology," in *J. Phys. Conf. S.*, vol. 2872, no. 1, p. 012003, 2024. [CrossRef]
21. M. R. Habibi, J. M. Guerrero, and J. C. Vasquez, "Artificial intelligence for cybersecurity monitoring of cyber-physical power electronic converters: A DC/DC power converter case study," *Sci. Rep.*, vol. 14, no. 1, p. 22072, 2024. [CrossRef]
22. J. Li, H. Gao, and Y. Wang, "Design of fuzzy delay compensation controller based on amplitude compensation method for power system with communication delay," *Int. J. Fuzzy Syst.*, vol. 27, no. 2, pp. 1–23, 2024.
23. Z. Shi, J. Fu, Z. Kang, and Y. Liang, "Noise mitigation method for power line communication based on cross-correlation analysis," in *J. Phys. Conf. S.*, vol. 2846, no. 1, p. 012020, 2024. [CrossRef]
24. X. Li, W. Li, N. Wang, L. Li, and X. Gong, "Resilience enhancement by line hardening for communication routing considering renewable energy sources in cyber-physical power systems," *IET Renew. Power Gener.*, vol. 18, no. 14, pp. 2477–2495, 2024. [CrossRef]
25. Z. Shams, and M. Rahmani, "Distributed observer for fault estimation in load-frequency control of multi-area power systems with communication delays," *J. Franklin Inst.*, vol. 361, no. 15, p. 107134, 2024. [CrossRef]
26. X. Liu, Y. Li, and T. Xu, "Impact of communication link overload on power flow and data transmission in cyber–physical power systems," *Electronics*, vol. 13, no. 15, p. 3065, 2024. [CrossRef]
27. F. Liu, J. Liu, Y. Bian, and Q. Geng, "Cascaded H-bridge power carrier communication method based on harmonic injection," in *J. Phys. Conf. S.*, vol. 2814, no. 1, p. 012063, 2024. [CrossRef]
28. Y. Qin, X. Lin, and J. Huang, "Low-delay low-voltage load aggregator demand response communication transmission architecture based on 5G edge computing," in *J. Phys. Conf. S.*, vol. 2831, no. 1, p. 012009, 2024. [CrossRef]
29. Q. Su, H. Guo, and J. Li, "A new model of electrical cyber–physical systems considering stochastic communication link failures," *J. Franklin Inst.*, vol. 361, no. 14, p. 107069, 2024. [CrossRef]
30. S. Avram, and R. Vasiu, "Optimal passive power line communication filter for NB-PLC applications," *Electronics*, vol. 13, no. 15, p. 2920, 2024. [CrossRef]
31. D. K. Belete, and A. O. Salau, "Adaptation and performance evaluation of existing power line for broadband communication," *Wirel. Personal Commun.*, vol. 137, no. 1, pp. 237–257, 2024. [CrossRef]
32. H. Yu, W. Gao, and K. Zhang, "A graph reinforcement learning-based handover strategy for low earth orbit satellites under power grid scenarios," *Aerospace*, vol. 11, no. 7, p. 511, 2024. [CrossRef]
33. X. Huang, L. Li, W. Wang, L. Liu, and M. Li, "Intelligent patrol inspection of low-code enabled electric power communication equipment based on digital transformation," *Clust. Comput.*, vol. 27, no. 8, pp. 10421–10435, 2024. [CrossRef]
34. L. Zhu, Q. Yang, and S. Ding, "Delay analysis of UAV networks with hybrid wireless and power line communication," *IEICE Commun. Express*, vol. 13, no. 4, pp. 110–113, 2024. [CrossRef]
35. N. Daldal, O. Aytar, E. Bekiroglu, and G. Bal, "Design and implementation of drive and control system for ultrasonic motor over power line communication," *Electr. Power Compon. Syst.*, vol. 52, no. 7, pp. 1082–1093, 2024. [CrossRef]
36. Z. Wan, L. Lin, Y. Huang, and X. Wang, "A graph neural network based fault diagnosis strategy for power communication networks," *J. Chin. Inst. Eng.*, vol. 47, no. 3, pp. 273–282, 2024. [CrossRef]

Yong Zhang, born in 1980, is a seasoned expert in the field of power information and communication. Born and raised in Kaifeng, Henan, his passion for information and communication led him to pursue a degree in Communication Engineering at Xidian University, where he earned his bachelor's degree in 2003. Zhang began his career in 2003, working tirelessly for 22 years at the Henan Electric Power Company, where he managed and operated the power information and communication system. During his tenure, he held various positions and made significant contributions to the safe and stable operation of the Henan power information and communication network.

Yan Liu, born and raised in Jiyuan, Henan, is a seasoned engineer in the field of power information and communication. Her passion for information and communication led her to pursue a degree in communication engineering at Wuhan University, where she earned her bachelor's degree in 2017. She then began working at the Henan Electric Power Company, focusing on the operation and management of power communication systems. Her work has significantly contributed to the safe and stable operation of Henan's power information and communication network.

Chunying Wang, born and raised in Nanyang, Henan province, is a senior expert in the field of power communication. She received her master's degree from Fuzhou University in 2012 and began to work in the operation and management of power communication system of Henan Electric Power Company in the same year. She has made significant contributions to the safe and stable operation of Henan electric power communication network.

Jiaojiao Dong, born and raised in Pingdingshan, Henan province, is a senior expert in the field of power communication. She received her master's degree from Beijing Institute of Technology in 2020 and began to work in the operation and management of power communication system of Henan Electric Power Company in the same year. She has made significant contributions to the safe and stable operation of Henan electric power communication network.